Brain Structure and Function
https://doi.org/10.1007/s00429-017-1594-9

ORIGINAL ARTICLE

Plasticity in deep and superficial white matter: a DTI study in world class gymnasts

Feng Deng[1] · Ling Zhao[1] · Chunlei Liu[2,3] · Min Lu[4] · Shufei Zhang[1] · Huiyuan Huang[1] · Lixiang Chen[1] · Xiaoyan Wu[1] · Chen Niu[1] · Yuan He[1] · Jun Wang[5] · Ruiwang Huang[1]

Received: 3 October 2017 / Accepted: 12 December 2017

Abstract

Brain white matter (WM) could be generally categorized into two types, deep and superficial WM. Studies combining these two types WM are important for a better understanding of brain plasticity induced by motor training. In this study, we applied both univariate and multivariate approaches to study gymnastic training-induced plasticity in brain WM. Specifically, we acquired diffusion tensor imaging data from 13 world class gymnasts and 14 non-athlete normal controls, reconstructed brain deep and superficial WM tracts, estimated and compared their fractional anisotropy (FA) difference between the two groups. Taking FA values as the features, we applied logistic regression and support vector machine to distinguish the gymnasts from the controls. Compared to the controls, the gymnasts showed lower FA in four regional deep WM tracts, including the occipital lobe portion of left inferior fronto-occipital fasciculus (IFOF.L), occipital and temporal lobe portion of right inferior longitudinal fasciculus (ILF.R), insular cortex portion of right uncinate fasciculus (UF.R), and parietal lobe portion of right arcuate fasciculus (AF.R). Meanwhile, we found lower FA in the superficial U-shaped tracts within the frontal lobe in the gymnasts compared to the controls. In addition, we detected that mean FA in either the AF.R or the U-shaped tracts connecting the left pars triangularis and superior frontal gyrus was negatively correlated with years of training in the gymnasts. Classification analyses indicated FA in deep WM hold higher potential to distinguish the gymnasts from the controls. Overall, our findings provide a more complete picture of training-induced plasticity in brain WM.

Keywords Neuroplasticity · Tractography · Logistic regression · Support vector machine (SVM)

Electronic supplementary material The online version of this article (https://doi.org/10.1007/s00429-017-1594-9) contains supplementary material, which is available to authorized users.

✉ Ruiwang Huang
ruiwang.huang@gmail.com

[1] Institute for Brain Research and Rehabilitation, Guangdong Key Laboratory of Mental Health and Cognitive Science, Center for Studies of Psychological Application, School of Psychology, South China Normal University, Guangzhou 510631, People's Republic of China

[2] Department of Electrical Engineering and Computer Sciences, University of California, Berkeley, CA 94720, USA

[3] Helen Wills Neuroscience Institute, University of California, Berkeley, CA 94720, USA

[4] CAS Key Laboratory of Mental Health, Institute of Psychology, Chinese Academy of Sciences, Beijing 100101, People's Republic of China

[5] State Key Laboratory of Cognitive Neuroscience and Learning and IDG/McGovern Institute for Brain Research, Beijing Normal University, Beijing 100875, People's Republic of China

Abbreviations

ATR	anterior thalamic radiation
CST	corticospinal tract
CGC	cingulum cingulate
IFOF	Inferior fronto-occipital fasciculus
ILF	Inferiorlongitudinal fasciculus
SLF	Superior longitudinal fasciculus
UF	Uncinate fasciculus
AF	Arcuate fasciculus
Tr	Pars triangularis
SF	Superior frontal
RMF	Rostralmiddle frontal
Op	Pars opercularis
WCGs	World class gymnasts
NCs	Non-athletenormal controls
FA	Fractional anisotropy
WM	Gray matter
GM	Gray matter

Published online: 18 December 2017

Introduction

Environmental enrichment can change the anatomical composition and function of the brain (Bennett et al. 1964; Draganski et al. 2004; Scholz et al. 2009; Zatorre et al. 2012). It is now widely accepted that, through the lifespan, the brain neuroanatomy maintains a capacity to reshape and reorganize in response to physical and cognitive activity (Sexton et al. 2016; Hartzell et al. 2016). Studies revealing plasticity-related mechanisms induced by physical and cognitive exercise in humans and animals are much needed. In this context, athletes become a useful model for investigating physical training-induced neuroplasticity in human brain (Wang et al. 2013; Hänggi et al. 2015; Huang et al. 2015; Park et al. 2015). Gymnastics is a competitive sport that requires precise motor control, balance, power, physical strength, flexibility and attention during the execution of motions. World class gymnasts (WCGs) who participate in long-term training, often start training very early in childhood and maintain it throughout their entire careers, have extraordinary performance in gymnastics competition and are thus excellent candidates for studying neuroplastic change induced by motor training in the human brain (Wang et al. 2013; Huang et al. 2015).

Diffusion tensor imaging (DTI) is the only available non-invasive technique to date to study neuroplasticity in macroscopic brain connections in vivo (Pierpaoli et al. 2001; Jbabdi et al. 2015; Lerch et al. 2017). Brain white matter (WM) could be generally categorized into two types, deep white mater (deep-WM) and superficial white mater (super-WM).With the newly developed DTI technique (Jones 2010), the major deep-WM tracts (Reveley 2015; Johnson et al. 2014; Lebel et al. 2012; Johansenberg and Rushworth 2009) have been widely studied and several methods (such as deterministic and probabilistic tractography) have been developed to extract these tracts in human brain. In contrast, the short-range U-shaped tracts of super-WM have been rarely studied (Reveley 2015). Super-WM tracts form connections between adjacent gyri in cerebral cortex and thus mediate communication between cortical association areas (Oishi et al. 2011; Schüz et al. 2002; Catani et al. 2012). They leave the cortex and follow its folding within the underlying thin layer and then reenter the cortex. Super-WM tracts are the slowest fiber tracts to myelinate within the nervous system and myelination may extend into the fourth decade of life (Barkovich 2000; Maricich et al. 2007), which may result in high plasticity.

Training-induced neuroplasticity in human brain have been identified in the deep-WM tracts. For examples, Huang et al. (2015) found decreased fractional anisotropy (FA) in bilateral superior longitudinal fasciculus (SLF), inferior longitudinal fasciculus (ILF), and inferior fronto-occipital fasciculus (IFOF) in the WCGs compared to non-athlete normal controls. Wang et al. (2014) found bilateral upper extremity motor skill training increased FA in the posterior and anterior limbs of the internal capsule, the corona radiate, and the body of the corpus callosum. Noticeably, those findings were derived from either voxel-wise (e.g., TBSS) or ROI-wise (mean value across the entire major deep-WM tracts) analyses. Actually, voxel-wise comparison could not tell information about properties of WM fiber tracts and due to the fact that small bundles join and leave larger fasciculus (Jbabdi and Johansen-Berg 2011), mean values across the entire deep-WM tracts may be insufficiently sensitive to detect the regional change in the long-range deep-WM tracts (Johnson et al. 2014; Yeatman et al. 2012, 2014). Thus, the first question we try to answer is whether gymnastic training induces regional plastic change in long-range deep-WM tracts. To answer this question, we applied a finer grained analysis procedure which could preserve information at different location on the long-range deep-WM tracts (Yeatman et al. 2012).

Studies have suggested the importance of super-WM tracts in the local connectivity and in the cognitive functions. For example, super-WM is being increasingly recognized in a variety of functions, such as working memory (Nazeri 2013), processing speed (Nazeri 2013), and visuomotor attention (Nazeri et al. 2015). So far, very few studies have explored brain neuroplasticity in super-WM tracts. Several studies found training-induced change in super-WM even though they did not focus on or recognize it as super-WM. For example, juggling training induced increased FA in WM underlying intra parietal sulcus (Scholz et al. 2009), complex visuomotor rotation training induced increased FA below the primary motor cortex (Landi et al. 2011), and complex whole-body balance task led to decreased FA in prefrontal WM regions (Taubert et al. 2010). Thus, the second question we focused on is whether gymnastic training induces plastic change in the super-WM tracts. As group-wise comparisons of super-WM structures is difficult with tractography because of high inter-individual variability (Oishi et al. 2008), to answer this question, we followed a procedure described by Nazeri et al. (2015), who designed a 2-step method which combined probabilistic tractography with TBSS pipelines (Smith et al. 2006). This method permits specific voxel-wise examination of the super-WM tracts across the brain and enhances between-subject registration of these tracts.

To have a better description of gymnastic training-induced neuroplasticity in brain WM tracts, we reconstructed long-range deep-WM and short-range super-WM tracts and applied between-group analyses by combing univariate and multivariate analytical approaches. The aims were to: (1) assess the group difference in diffusion

properties of the deep- and super-WM tracts between the gymnasts and the non-athlete normal controls (NCs), (2) assess the relationship between the brain structural change and years of training, and (3) determine the relative contribution of the deep- and super-WM in distinguishing the gymnasts from the controls.

Methods

Subjects

We recruited 13 right-handed world class gymnasts (WCGs 6 M/7 F, age 17–26 years, mean ± SD = 20.5 ± 3.2 years) from December 9, 2009 to December 27, 2009. Each of them had won at least one gold medal in the Gymnastics World Cup or the Olympic Games since 2007 (Table 1). They were still active in training/competition by the time of scanning. All of them had started gymnastic training at an age of about 4.5 years old and had more than 12.5 years of training experience with a mean training time of 6 h per day by the time of this experiment. We also recruited 14 age- and gender-matched right-handed non-athlete healthy subjects as the controls (NCs 7M/7F, age 19–28 years, mean ± SD = 22.6 ± 2.8 years). No significant between-group difference was found either in age ($t_{(25)} = -1.75$, $p = 0.09$) or in gender ($\chi^2_{(1)} = 0.04$, $p = 0.84$). All the subjects had at least high school level education at the time of scanning and none of the subjects had a history of neurological or psychiatric disorders or brain injuries. The study was approved by the Institutional Review Board of the State Key Laboratory of Cognitive Neuroscience and Learning at Beijing Normal University (BNU). Written informed consent was obtained from each subject prior to the study.

Data acquisition

DTI and 3D T_1-weighted brain structural images were acquired on a 3T Siemens Trio TIM MR scanner (Siemens Healthcare, Erlangen, Germany) with a 12-channel phased-array head coil. The foam pads and headphones were used to reduce head motion for each subject during the MRI data acquisition. All images were acquired using generalized auto-calibrating partially parallel acquisitions (GRAPPA) (Griswold et al. 2002) scheme with a reduction factor of 2 and 24 reference lines. DTI data were obtained using a twice-refocused spin-echo diffusion-weighted echo-planar imaging (EPI) sequence with following parameters: repetition time (TR) = 10,000 ms, echo time (TE) = 92 ms, 64 non-linear directions with $b = 1000$ s/mm^2 and one volume with $b = 0$, slice thickness = 2 mm without gap, field of view (FOV) = 256 × 248 mm, data matrix = 128 × 124, voxel size = 2 × 2 × 2 mm^3, 75 interleaved transverse slices (without interslice-gap) covering the whole brain. High-resolution brain structural images were acquired using the 3D T_1-weighted magnetization-prepared rapid gradient echo (MP-RAGE) sequence (TR = 1,900 ms, TE = 3.44 ms, inversion time = 900 ms, flip angle = 8°, 176 sagittal slices, FOV = 256 × 256 mm, matrix = 256 × 256, voxel size = 1 × 1 × 1 mm^3). For each subject, both DTI and MP-RAGE sequences were repeated three times in a single

Table 1 Demographic characteristics of the world class gymnasts

Gymnasts	Discipline	Best medal records since 2007	Gender	Age (years old)	Age of commencement (years old)	Years of training
1	Pommel horse	OC	M	24	4.5	19.5
2	Still rings	WC	M	24	4.5	19.5
3	Parallel bars	WC	M	23	4.5	18.5
4	Horizontal bar, AA	WC	M	26	4.5	21.5
5	Parallel bars, AA	WC	M	21	4.5	16.5
6	Pommel horse	WC	M	23	4.5	18.5
7	Uneven bars, AA	OC	F	18	3.5	14.5
8	Floor exercise	OC	F	17	4.5	12.5
9	Uneven bars, AA	OC	F	17	4.5	12.5
10	Uneven bars, AA	WC	F	17	4.5	12.5
11	Uneven bars, AA	WC	F	19	4.5	14.5
12	Vault	OC	F	21	4.5	16.5
13	Balance beam, AA	OC	F	17	4.5	12.5
Mean ± SD				20.5 ± 3.2	4.4 ± 0.3	16.1 ± 3.2

Mean and SD are reported unless otherwise specified

OC Olympic Champions; *WC* World Champions or World-Cup Champions; *AA* all around; *SD* standard deviation; *M* male; *F* female

session with a total scan time of about 50 min. Three DTI scans were averaged in the preprocessing step to increase the signal-to-noise ratio (SNR). We visually checked all the images on site and found that all showed good image quality.

Data preprocessing

For each subject, the three DTI datasets were concatenated together and the effects of head motion and image distortions caused by eddy-currents were corrected using the FSL/FDT (Jenkinson et al. 2012) by applying the affine alignment of all diffusion-weighted images (64×3 volumes) to the averaged $b = 0$ volumes (1×3 volumes). Diffusion encoding gradients were adjusted to account for the rotation applied to the measurements during motion correction (Alexander et al. 2001). The head motion corrected dataset was split into three DTI datasets, corresponding to the three original DTI scans, which were averaged to generate one DTI dataset of 65 volumes. Subsequently, a tensor model was used to fit the averaged data. Four diffusion measures, fractional anisotropy (FA), axial diffusivity (AD), radial diffusivity (RD), and mean diffusivity (MD), were computed using eigenvalues (λ_1, λ_2, and λ_3) in each voxel.

Since the deep- and super-WM embraced different characteristics, such as range, size, and variability across different subjects, we applied two different methods to reconstruct the deep- and super-WM tracts separately. We used the automated fiber-tract quantification (AFQ) for reconstruction of the deep-WM tracts (Yeatman et al. 2012) and the probabilistic tractography combined with modified TBSS pipelines for reconstruction of the super-WM tracts (Nazeri et al. 2015).

Deep white matter tracts

An automated fiber-tract quantification (AFQ) analysis pipeline (Yeatman et al. 2012) was used to identify brain deep-WM tracts for each subject. We segmented the brain deep-WM into 18 major tracts which are defined according to a WM atlas (Wakana et al. 2007). Primarily, the processing pipelines consists of six steps: (1) whole-brain fiber tractography using a deterministic streamlines tracking algorithm (thresholds: FA > 0.2 and turning angle < 30°), (2) waypoint ROI-based tract segmentation using the anatomical descriptions (Wakana et al. 2007), (3) fiber refinement according to the fiber tract probabilistic maps (Hua et al. 2008), (4) fiber-tract cleaning using a statistical outlier rejection algorithm (Yeatman et al. 2012), (5) fiber tract clipping to the central portion that spans between the two defining ROIs, and (6) quantification of the diffusion measures at 100 equidistant nodes along each fiber tract. In step 4, we sampled each fiber in a fiber group at 100 equidistant nodes, represented the spread of fibers at each node as a 3D Gaussian distribution, and removed any fiber that is more than five standard deviation from the core of the fiber group. The fiber core is calculated as the mean of each fiber's coordinates at each node. This procedure was repeated until no more fiber outliers appear. In step 6, diffusion measures were calculated along the trajectory of a fiber group by interpolating values (FA, MD, AD, and RD) at each node along each fiber. Diffusion 'Tract Profiles' of each measure were then calculated as a weighted sum of each fiber's value at a given node where a fiber is weighted based on its Mahalanobis distance from the core location of the tract as:

$$D_{\mathrm{m}}(x) = \sqrt{(x-u)^T S^{-1} (x-u)^T}, \quad (1)$$

where $\boldsymbol{x}$ is a vector containing a fiber node's coordinate, u represents mean coordinate of each node on the fiber group, and S means a 3×3 covariance matrix of spread of fibers on each node.

Actually, the AFQ procedure may not identify all 18 deep-WM tracts in each subject. In specific, using AFQ, we failed to identify the left cingulum cingulate (CGC) in one of the 13 gymnasts and the right arcuate fasciculus (AF) in one of the 14 control subjects. For the other subjects, the AFQ identified all 18 WM tracts in this study.

Superficial white matter tracts

The super-WM tracts were assessed via a combination of probabilistic tractography and modified TBSS pipelines. We first performed the conventional TBSS pipelines (FSL/TBSS) (Smith et al. 2006) for the preparation of next analyses. The procedures were described as follows.

Creation of superficial white matter mask

For each subject, probabilistic tractography was performed within the native diffusion space using FSL/FDT. To constrain tractography within the super-WM, we carried out the following three-step analyses: (1) cortical reconstruction, the T_1-weighted structural images were processed with FreeSurfer v5.3.0 (https://surfer.nmr.mgh.harvard.edu/) to determine GM/WM boundary of bilateral hemispheres which were affinely (12-parameter linear transform) aligned to the native diffusion space using FLIRT/FSL (Jenkinson and Smith 2001). Meanwhile, the deep-WM mask, which is binary Johns Hopkins University DTI-atlas (http://fsl.fmrib.ox.ac.uk/fsl/fslwiki/Atlases), was nonlinearly registered to the native diffusion space using the inverted transformation fields generated during conventional TBSS pipelines, (2) probabilistic tractography, this step was conducted via FSL/bedpostX/probtrackX (Behrens et al. 2003, 2007). We first used BedpostX, a 2-tensor model, to create the distributions of diffusion parameters by running Markov Chain

Monte Carlo sampling at any given voxel. Then based on the output of bedpostX, we performed probabilistic tractography to reconstruct the super-WM tracts. In this step, we performed tractography seeded from the cortical GM/WM boundary and discarded streamlines passing through the deep-WM mask, (3) streamline normalization, the obtained streamlines of the super-WM tracts for each individual were first normalized by the total number of successfully traced streamlines (the "waytotal") and then were thresholded at 0.01% of waytotal. Next, the super-WM mask, which is binarization of individual super-WM tracts, was performed and nonlinearly transformed to the MNI standard space using transformation fields generated from conventional TBSS pipelines. Finally, all subjects' super-WM masks were averaged to generate a probabilistic group super-WM mask which was thresholded at 50%.

Modified TBSS analysis

The mean FA image, which is the averaged FA images across all subjects obtained from the conventional TBSS pipelines, was multiplied by the thresholded probabilistic group super-WM mask to generate a new mean FA image which was constrained within this super-WM mask. A "thinning" procedure, which is similar to conventional TBSS pipelines, was applied to the new mean FA image of super-WM to create a skeletonized mean FA image. Non-WM voxels were discarded from the skeleton by thresholding the skeletonized mean FA image of super-WM ($FA > 0.2$). To account for residual misalignments and facilitate group-wise comparison, we searched each individual FA image orthogonal to the skeleton by setting the thresholded probabilistic group super-WM mask as the constrained search space. The local maxima of FA, which represent the centers of the super-WM tracts, were detected in the MNI space and then projected back onto the individual skeleton.

Statistical analyses

Group comparisons of diffusion measures

A non-parametric permutation test (Nichols and Holmes 2002) was used to detect between-group difference of $FA_{deep-WM}$ (FA in deep white matter) and $FA_{super-WM}$ (FA in superficial white matter) separately. For each deep-WM tract, we calculated the group effect of node-wise difference in FA tract profiles to depict FA change in the regional deep-WM tracts and also determined the mean FA across an entire fiber tract. In addition, we calculated group effect of node-wise difference in MD, AD and RD tract profiles for each of the deep-WM tracts. Similarly, the group difference in FA was also estimated for the super-WM tracts. In the calculations, we adopted FSL/randomise (5000 permutations) and selected threshold-free cluster enhancement (TFCE) to provide brain-wide significance. Potential confounding variables (age and gender) were controlled for group comparisons. To correct for false positives rate resulted from multiple comparisons across 100 nodes along the deep-WM tracts or from voxel-wise comparisons within the super-WM tracts, we implemented a false discovery rate (FDR) correction procedure ($q = 0.05$) (Benjamini and Hochberg 1995).

Brain-behavior correlations

In the gymnastic group, we conducted brain-behavior correlation analyses for the deep- and super-WM tracts separately. For each of the deep-WM tracts showing significant group difference, we calculated the correlation between years of training and FA tract profiles to form a new vector called "behavioral tract profiles". The FDR correction procedure ($q = 0.05$) (Benjamini and Hochberg 1995) was used to correct for multiple comparisons. In addition, we also estimated correlations between the mean FA across the entire deep-WM tracts showing significant group difference and years of training. For the super-WM, we first determined the mean FA of each cluster showing significant group difference for each gymnast and then estimated the correlation between the mean FA and years of training. In the calculations, we took age and gender as confounding variables. Pearson's correlation coefficient was used to depict the degree of correlation.

Classification based on deep and superficial white matter

We built several classifiers which take features (independent variables or predictors) of an example (the FA values in deep- and super-WM) and predict the class that example belongs to (the dependent variable). $FA_{deep-WM}$ and $FA_{super-WM}$ were served as independent variables to detect the relative contributions of the deep- and super-WM to predict the two classes, the gymnasts and the controls (the dependent variable) with logistic regression and linear support vector machines (SVM). Logistic regression and SVM are two frequently-used linear classifiers, which tend to be roughly equivalent in terms of performance although they are different in classifier construction (Pereira and Botvinick 2009).

In the logistic regression analysis, we selected two candidate independent variables, the mean $FA_{deep-WM}$ and mean $FA_{super-WM}$, for each subject separately. Two methods, the likelihood ratio (LR) stepwise forward method and the Enter method, were adopted to construct classifiers. That is, we adopted the LR and Enter methods for selecting these independent variables into the following regression equation:

$$\text{logit}(p) = \log\left(\frac{p(y=1)}{1-p(y=1)}\right) = \beta_0 + \beta_1 x_1 + \beta_2 x_2 + \cdots + \beta_n x_n, \quad (2)$$

where logit(p) means the log-odds of an event, y represents the class and p is the probability of the odds ($0 < p < 1$). β_0 represents the constant term. x_1, x_2, …, and x_n are independent variables. β_1, β_2, …, and β_n are the regression coefficients corresponding to the independent variables. The LR stepwise forward method means that we set the criteria first through calculation, and then selected any candidate variable meeting the criteria into Eq. 2. While for the Enter method, we put all candidate independent variables into Eq. 2 without setting any criteria first. In specific, we selected $n = 2$, $x_1 = \mathrm{FA}_{\mathrm{deep-WM}}$, and $x_2 = \mathrm{FA}_{\mathrm{super-WM}}$ in this study and the logistic regression analysis was processed using SPSS version 22.0 (IBM Corp 2011).

The SVM analysis was processed using the MANIA toolbox (Grotegerd et al. 2014) and LIBSVM (a library for support vector machines) (Chang and Lin 2011). In the calculations, we treated individual FA map in the standard space as feature to build classifiers to distinguish the two groups. We first produced three masks, super-WM skeleton mask, deep-WM mask which is a binary ICBM-DTI-81 white matter labels atlas (Szeszko and Kingsley 2010), and a combination mask of the deep- and super-WM, and then used them to detect the relative importance of the deep- and super-WM in the performance of classifiers, The cross-validation was performed using the leave-one-subject-out cross-validation (LOOCV) approach in which a feature ranking method using F tests based on a probability ($p < 0.05$) was embedded. A non-parametric permutation test was used to determine statistical significance (100 permutations) at the significant level of $p < 0.05$.

Results

Comparisons of tract profiles

Figure 1 shows FA tract profiles and Table 2 lists the mean FA of the 18 major deep-WM tracts of the gymnasts and the controls.

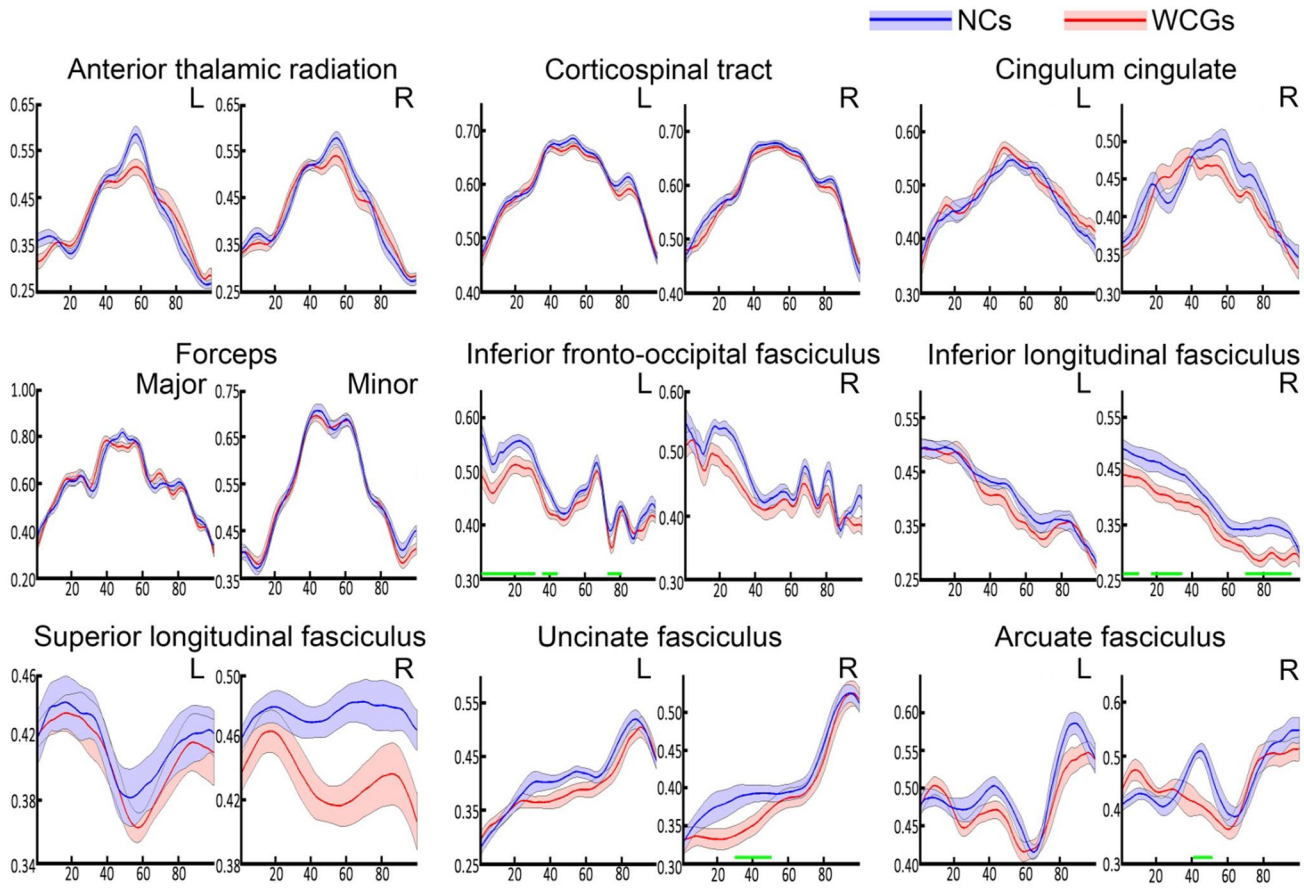

Fig. 1 Node-wise and mean fractional anisotropy (FA) along the 18 identified deep white matter tract profiles between the world class gymnastics (WCGs) and the non-athlete normal controls (NCs). The FA tract profiles are presented in mean ± standard error (SE). The red curve stands for the WCGs and the blue for the NCs. The solid curves stand for the mean values across each deep-WM tract and the shaded areas for SE. The green bars under the FA profiles indicate the regions showing significant group difference in FA. The horizontal axis indicates the location between the beginning and termination waypoint region of interest along the given tract, while the vertical axis indicates FA value. Similarly, the red stands for the WCGs and the blue for the NCs. Abbreviation: *L* (*R*), left (right) hemisphere

Table 2 Mean fractional anisotropy (FA) of deep white matter tracts in the world class gymnasts (WCGs) and the non-athlete normal controls (NCs)

Index	Tracts	WCGs	NCs	*p* value
1	ATR.L	0.41 (0.03)	0.41 (0.03)	0.49
2	ATR.R	0.42 (0.02)	0.43 (0.02)	0.41
3	CST.L	0.60 (0.02)	0.60 (0.02)	0.29
4	CST.R	0.59 (0.02)	0.59 (0.02)	0.22
5	CGC.L	0.48 (0.03)	0.47 (0.03)	0.17
6	CGC.R	0.42 (0.03)	0.43 (0.03)	0.26
7	Forceps major	0.60 (0.03)	0.60 (0.03)	0.33
8	Forceps minor	0.53 (0.03)	0.54 (0.03)	0.35
9	IFOF.L	0.45 (0.02)	0.47 (0.02)	1.99E − 04
10	IFOF.R	0.44 (0.02)	0.46 (0.02)	0.01
11	ILF.L	0.40 (0.03)	0.41 (0.02)	0.14
12	ILF.R	0.36 (0.04)	0.40 (0.04)	0.01
13	SLF.L	0.41 (0.03)	0.42 (0.05)	0.32
14	SLF.R	0.43 (0.04)	0.48 (0.03)	0.01
15	UF.L	0.39 (0.03)	0.41 (0.03)	0.07
16	UF.R	0.39 (0.03)	0.41 (0.03)	0.01
17	AF.L	0.48 (0.03)	0.49 (0.02)	0.01
18	AF.R	0.44 (0.04)	0.46 (0.03)	0.06

The between-group comparisons were conducted by averaging 100 nodes along the tract length (5,000 permutations). Mean and standard deviation (SD) of diffusion measures are reported unless otherwise specified

ATR anterior thalamic radiation; *CST* corticospinal tract; *CGC* cingulum cingulate; *IFOF* inferior fronto-occipital fasciculus; *ILF* inferior longitudinal fasciculus; *SLF* superior longitudinal fasciculus; *UF* left uncinate fasciculus; *AF* arcuate fasciculus; *FA* fractional anisotropy; *L* (*R*) left (right) hemisphere

Figure 2 shows regional difference of FA tract profiles between the gymnasts and the controls. Using the node-wise comparison, we found four tract profiles in total, the left IFOF, right ILF, UF and AF, showing regionally lower FA in the gymnasts compared to the controls. Specifically, in the posterior portion (adjacent to the occipital lobe) of the left IFOF (at the peak node, mean FA across all WCGs, $FA_{WCGs} = 0.45$, mean FA across all NCs, $FA_{NCs} = 0.57$, $p = 0.001$, FDR corrected), in both the temporal and occipital lobe extension of the right ILF (at the peak node, $FA_{WCGs} = 0.29$, $FA_{NCs} = 0.35$, $p = 0.001$, FDR corrected), in the insular cortex extension of the right UF (at the peak node, $FA_{WCGs} = 0.36$, $FA_{NCs} = 0.39$, $p = 0.001$, FDR corrected), and in the parietal lobe extension of the right AF (at the peak node, $FA_{WCGs} = 0.41$, $FA_{NCs} = 0.51$, $p = 0.0002$, FDR corrected), FA was significantly lower in the gymnasts compared to the controls. Detailed information about the group comparisons of diffusion tract profiles for each of the 18 major deep-WM tracts are listed in Tables S1 (Supplementary materials).

Our results also showed significantly lower mean FA in several tracts, three of them showed regional difference in the gymnasts compared to the controls, that is mean FA of the left IFOF ($FA_{WCGs} = 0.45$, $FA_{NCs} = 0.47$, $p = 1.99e\text{-}04$), the right ILF ($FA_{WCGs} = 0.36$, $FA_{NCs} = 0.40$, $p = 0.012$), the right UF ($FA_{WCGs} = 0.39$, $FA_{NCs} = 0.41$, $p = 0.013$). However, no significant difference in mean FA was found in the right AF between the gymnasts and the controls ($FA_{WCGs} = 0.44$, $FA_{NCs} = 0.46$, $p = 0.06$).

In addition, we found lower FA, while higher MD and RD, in tract profiles of the right ILF and the right UF in the gymnasts compared with the controls. In tract profile of the right AF, both FA and AD were lower in the gymnasts compared to the controls (Fig. S1 in Supplementary Materials).

Comparisons of superficial white matter

Figure 3 shows the locations of super-WM tracts with significant group difference in $FA_{super-WM}$ between the gymnasts and the controls ($q_{FDR} < 0.05$). There are four clusters located in the frontal lobe, including the bilateral fiber tracts connecting pars triangularis (Tr) and superior frontal cortex (SF), the right fiber tract connecting rostral middle frontal cortex (RMF) and SF, and the left fiber tract connecting pars opercularis (Op) and SF (Table 3).

Brain-behavior correlation in the gymnasts

Figure 4 shows that both $FA_{deep-WM}$ and $FA_{super-WM}$ were correlated to years of training. For the deep-WM tracts, we found that the mean FA of AF.R was negatively correlated with years of training ($r = -0.67$, $p = 0.026$, Fig. 4a). For the super-WM tracts, FA of one cluster, which is located in the left tract connecting Tr and SF, was significantly correlated with the training years ($r = -0.62$, $p = 0.040$, Fig. 4 b).

Classifications

Table 4 lists the results of classifications derived from the logistic regression. Using the LR stepwise forward approach, we only selected $x_1 = FA_{deep-WM}$ in Eq. 2 and obtained $\text{logit}^{LR}(p) = -47.74 + 102.90 \times FA_{deep-WM}$, that is $\beta_0 = -47.74$, $\beta_1 = 102.90$, and $\beta_2 = 0$. Further analysis showed an accuracy of 77.8% (sensitivity = 76.9%; specificity = 78.6%) to differentiate the two groups. Wald test shows that β_1 was significant (Wald = 5.99, $p = 0.01$), Omnibus test shows that the above expression $\text{logit}^{LR}(p)$ was significant ($\chi^2 = 8.64$, $p = 0.003$), and Hosmer–Lemeshow test shows that the above expression $\text{logit}^{LR}(p)$ has good fitness for the data ($\chi^2 = 5.10$, $p = 0.65$). In addition, the expression $\text{logit}^{LR}(p)$ showed that $FA_{deep-WM}$ could explain 37% (Na R^2) variance of dependent variable.

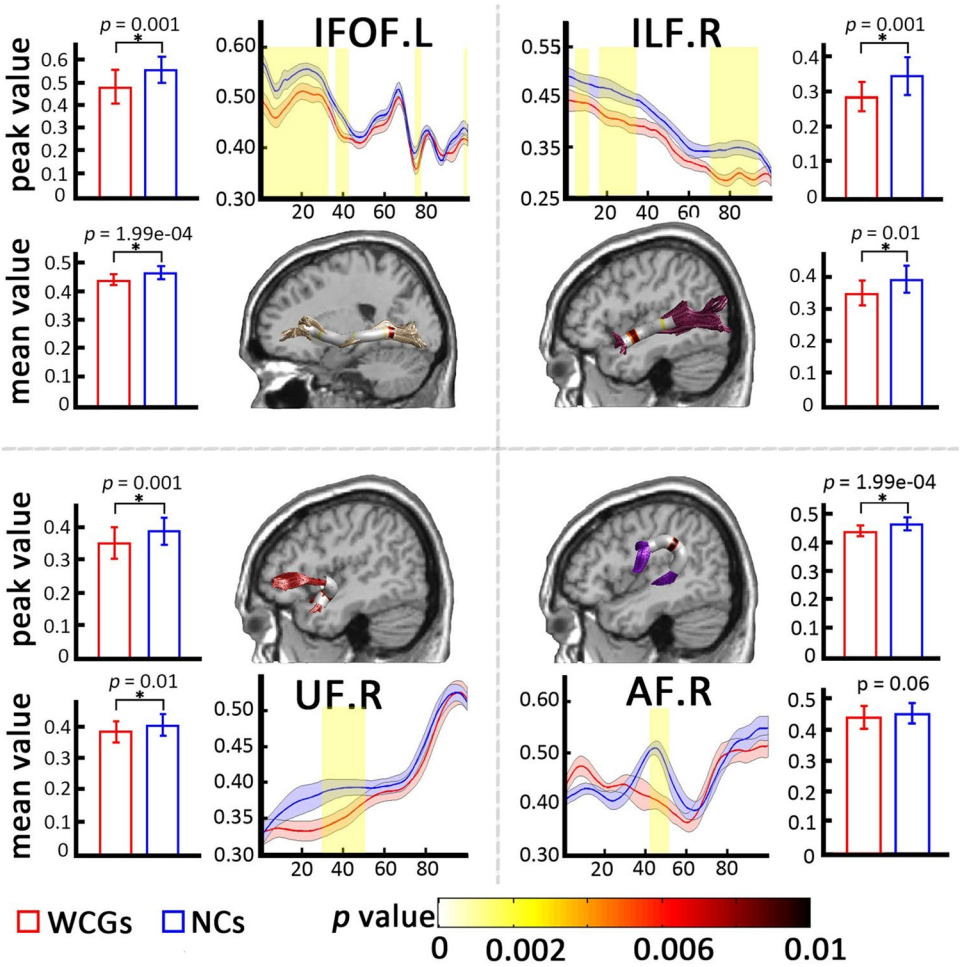

Fig. 2 Group comparison of FA tract profiles between the world class gymnasts (WCGs) and the non-athlete normal controls (NCs). The regional difference of the tract profiles are shown in a standard brain structure map. The non-white color means significant group difference. The color bar indicates *p* value of permutation tests conducted at each node along the tract length. The plots of FA tract profiles are presented with mean ± standard error (SE). The regions shaded with yellow color correspond to the regions showing significant between-group difference in FA values. The histogram shows the direction of FA change in peak values and mean values between the two groups. The red stands for the WCGs and the blue for the NCs. The peak values represent the location where the largest change occurred. The mean values represent group difference in the mean FA along the fiber tracts. Abbreviations: *IFOF.L* left inferior fronto-occipital fasciculus; *ILF.R* right inferior longitudinal fasciculus; *UF.R* right uncinate fasciculus; *AF.R* right arcuate fasciculus; *FA* fractional anisotropy

As for the Enter approach, we obtained $\text{logit}^{\text{Enter}}(p) = -43.62 + 111.51 \times FA_{\text{deep-WM}} - 21.02 \times FA_{\text{super-WM}}$ according to Eq. 2, that is, β_0 = -43.62, β_1 = 111.51, and β_2 = – 21.02. The above expression of $\text{logit}^{\text{Enter}}(p)$ was significant (Omnibus test, $\chi^2 = 8.86$, $p = 0.012$) and had a good fitness of the data (Hosmer–Lemeshow test, $\chi^2 = 5.45$, $p = 0.61$). The regression coefficient β_1 was significant (Wald = 5.50, $p = 0.02$) while β_2 was not significant (Wald = 0.21, $p = 0.64$). We noticed that even adding a new independent variable ($x_2 = \text{FA}_{\text{super-WM}}$) in Eq. 2, comparing $\text{logit}^{\text{Enter}}(p)$ to $\text{logit}^{\text{LR}}(p)$, it neither increased accuracy for distinguishing the two groups (accuracy = 74.10%) nor changed the explanation for variance of dependent variable (Na $R^2 = 37\%$).

Table 5 lists the results of classification obtained from SVM analysis. We found that $\text{FA}_{\text{deep-WM}}$ alone could result in the accuracy up to 81.48% (sensitivity = 84.62%; specificity = 78.57%) while $\text{FA}_{\text{super-WM}}$ alone could only result in an accuracy nearly at random level (51.85%) to distinguish the gymnasts from the controls. If we combined $\text{FA}_{\text{deep-WM}}$ and $\text{FA}_{\text{super-WM}}$ to perform the classification analysis, we could get a slightly lower accuracy (74.07%, sensitivity = 69.23%; specificity = 78.57%) to distinguish the two groups.

Discussion

We applied univariate and multivariate analyses to evaluate training-induced changes in regional deep-WM tracts as well as local super-WM tracts and the relative contributions of deep- and super-WM to distinguish the gymnasts from the controls. Our results from univariate analysis indicates long-term intensive gymnastic training could induce brain structure changes, both in specific long-range deep-WM tracts and short-range U-shaped tracts mainly connecting regions within frontal lobe. The results from multivariate analysis shows $\text{FA}_{\text{deep-WM}}$ had higher potential to distinguish the two groups than $\text{FA}_{\text{super-WM}}$.

Plasticity in deep white matter

We found lower mean FA in the bilateral IFOF, the right ILF, the right SLF, and the left AF in the gymnasts relative to the controls (Table 2), which is consistent with our previous research (Huang et al. 2015). AF is a part of the SLF (Makris et al. 2005; Petrides and Pandya 1984, 1988) and when reviewing their potential roles, we found the SLF and

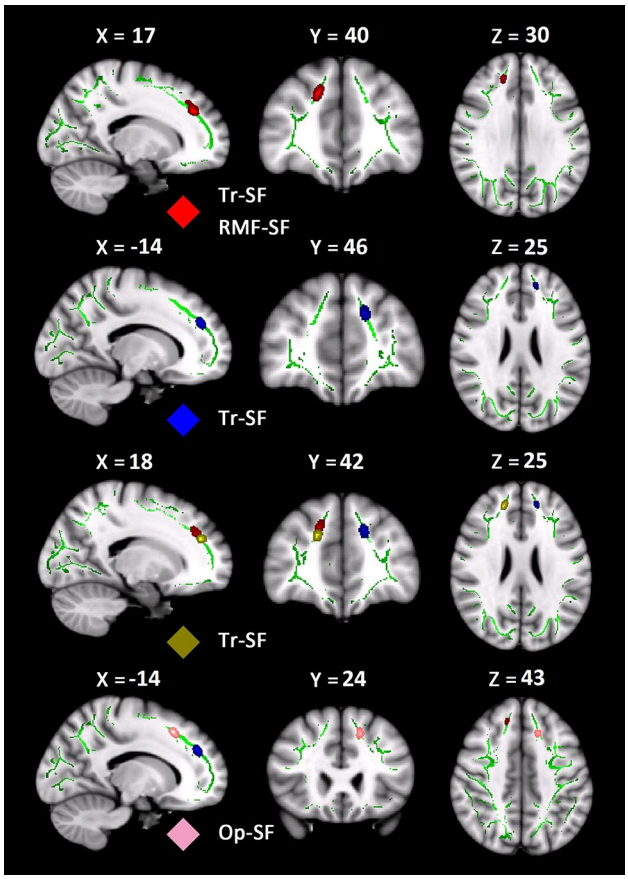

Fig. 3 Clusters derived from the modified tract-based spatial statistical analysis (TBSS) for superficial white matter (super-WM) showing lower fractional anisotropy (FA) in the world class gymnasts (WCGs) compared to the non-athlete normal controls (NCs) ($q_{FDR} < 0.05$). The white matter skeleton is projected (green) on the MNI-152 T1-w standard space (gray scale). The clusters indicate the brain areas with significant group difference, which are marked by red color (right Tr-SF and right RMF-SF), blue (left Tr-SF), yellow (right Tr-SF) and pink (left Op-SF). Radiological coordinate was applied. Abbreviations: *Tr* pars triangularis; *SF* superior frontal; *RMF* rostral middle frontal; *Op*, pars opercularis

the AF mainly contribute to visuospatial and auditory spatial information processing, especially in regulation of motor behavior, spatial attention and working memory (Makris et al. 2005; Umarova et al. 2010). Hoeft et al. pointed out that the ILF is associated with the ventral visual streams for object identification (Hoeft et al. 2007) and Schmahmann et al. suggested that the IFOF may be related to higher-order aspects of motor behavior and spatial attention (Schmahmann et al. 2007). Furthermore, Oechslin et al. (2009) demonstrated that the ILF, SLF, and IFOF are related to visuomotor processing and attention control. Taken together, our results showed that those functions essential for daily training of gymnasts, such as regulation of motor behavior and spatial attention, might relate to microstructural changes of those major deep-WM fasciculus. In addition, we found lower mean FA of the right UF in the gymnasts compared to the controls. A previous review suggested that the UF might be related to the expression of memory to guide decisions and to the acquisition of certain types of learning and memory (Von Der Heide et al. 2013). Thus, we infer that long-term and extensive gymnastic training, which requires quick stimuli discrimination and procedural memory extracting to make decision, may lead to the FA change in the right UF.

Gymnastic practice may cause either general WM maturation or with specific, localized WM changes due to the acquisition of a particular skill. In this study, we found the regional decreased FA alongside those major deep-WM tracts (Fig. 2). A possible explanation of the regional change in the deep-WM tracts is that the associated GM regions have an effect on these specific locations within major deep-WM tracts, such as generating axonal connections, which results in diffusion measure change at these locations (Konrad and Winterer 2008). Several longitudinal studies suggested that training-induced FA change in WM paralleled to density/volume change in corresponding GM areas (Scholz et al. 2009; Taubert et al. 2010). Thus, it is possible that our finding of FA change in regional locations of major deep-WM tracts is affected by change of associated GM areas. For example, FA change in parietal lobe portion of the right AF may be affected by density or/and volume change in parietal lobe. In fact, previous studies found increased GM volume in bilateral parietal lobule after a 2 weeks motor training (Filippi et al. 2010).

Alternately, the regional FA alteration in major deep-WM tracts may be caused by functional alteration in adjacent cortical regions since neuronal activity can regulate a series

Table 3 Clusters of superficial white matter with significantly decreased fractional anisotropy (FA) in the world class gymnasts (WCGs) compared to the non-athlete normal controls (NCs)

Clusters	Hemisphere	Cluster size (# voxels)	MNI coordinates			Mean FA (SD)		q_{FDR}
			X	*Y*	*Z*	WCGs	NCs	
Tr-SF, RMF-SF	Right	86	17	40	30	0.44 (0.02)	0.48 (0.03)	0.045
Tr-SF	Left	41	−14	46	25	0.42 (0.02)	0.47 (0.03)	0.045
Tr-SF	Right	28	18	42	25	0.44 (0.03)	0.48 (0.03)	0.045
Op-SF	Left	11	−14	24	43	0.50 (0.04)	0.57 (0.09)	0.045

The MNI coordinates correspond to the peak voxels of each cluster

Tr pars triangularis; *SF* superior frontal; *RMF* rostral middle frontal; *Op* pars opercularis

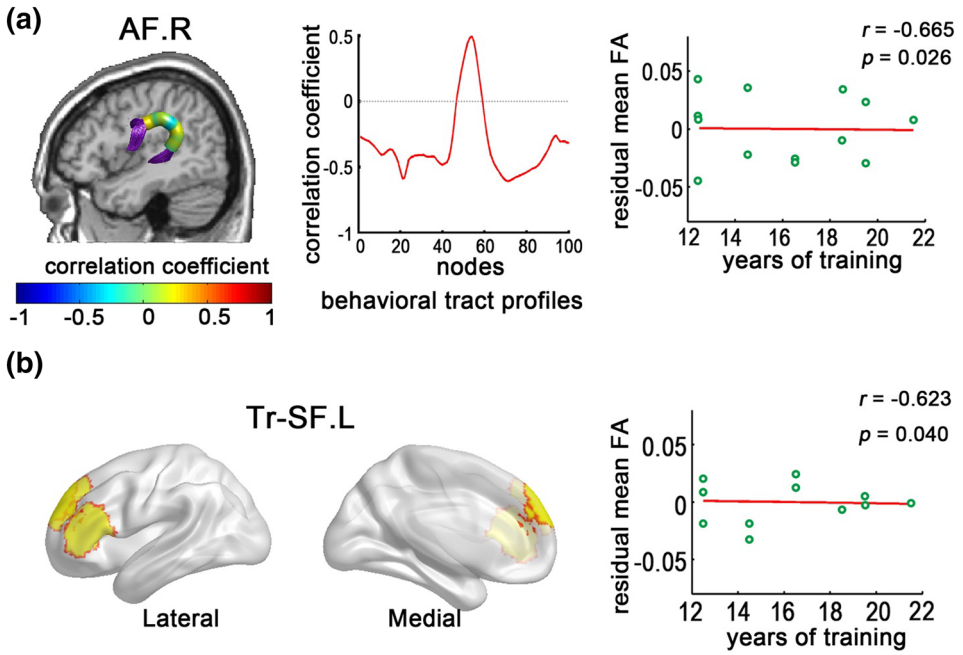

Fig. 4 Relationship between fractional anisotropy (FA) and years of training in the world class gymnasts (WCGs). **a** Behavioral tract profiles of AF.R. Color bar indicates Pearson's partial correlation between FA values and years of training which was conducted at each location along the tract length. The curve plot indicates the variation of correlation coefficients along the fiber tract. The scatter plot shows the correlations. **b** Brain regions showing the gray matter areas (Tr and SF) which are connected by the U-shaped fibers. The scatter plot shows mean FA (horizontal axis) changing with years of training (vertical axis) for a left U-shaped tract connecting Tr and SF. Abbreviations: *AF* arcuate fasciculus; *Tr* pars triangularis; *SF* superior frontal; *L* (*R*) left (right) hemisphere

of changes related to WM microstructure (Ishibashi et al. 2006). To be specific, we found lower FA in parietal lobe portion of the right AF in the gymnasts compared to the controls. The parietal lobe was found to code for spatial attention, contribute to the translation from visuospatial to body-related information during the acquisition of motor skills in human (Halsband and Lange 2006) and play a major role in visual aspects of spatial function in monkey (Bisley and Goldberg 2003). The posterior parietal cortex was found to relate to motor planning, sensory guidance of movements as well as higher-order aspects of motor control, such as coding the goal of action and linking action to perception (Fogassi and Luppino 2005). In addition, we found lower FA in posterior portion (near occipital areas) of the left IFOF and in occipital areas and anterior temporal portion of the right ILF in the gymnasts compared to the controls. The occipital gyrus is associated with visual information processing and the temporal gyrus is associated with multisensory integration, such as auditory and visual processing (Fan et al. 2014; Specht and Reul 2003). Furthermore, we found lower FA in insular cortex portion of the right UF in the gymnasts compared to the controls. The insular cortex is found to play a role of attentional switch between two functional networks, the default mode network and the executive control network (Menon and Uddin 2010), and thus might be related to quick preparation and alertness state in competition. And the posterior insula might be involved in processes of spatial exploration and orientation (Karnath et al. 2004).

Plasticity in superficial white matter

Microstructural change of the super-WM has less been reported and understood relative to that of cortical GM and deep-WM in the previous studies of motor skill training, especially in world class gymnasts. We found training-induced change of $FA_{super-WM}$ in the frontal lobe (Fig. 3), including four U-shaped tracts connected the SF (mainly in BA 6/8/9): the right RMF (BA 46)—SF, the right Tr-SF, the left Tr-SF, and the left Op-SF (Table 3). Phillips et al. found age-related reductions in FA that were more pronounced in the frontal super-WM than in the posterior and ventral brain regions, which suggested higher plasticity and vulnerability in the frontal super-WM (Phillips et al. 2013) and Nazeri et al. demonstrated that FA in super-WM adjacent to the right frontal lobe related to motor speed independent of FA in deep-WM (Nazeri et al. 2015). Our results corresponded to that of a previous study (Catani et al. 2012) which identified several U-shaped tracts located in the frontal lobe, including frontal aslant tract (FAT) connecting dorsal and medial (supplementary and pre-supplementary motor area,

Table 4 Logistic regression analysis using the mean fractional anisotropy (FA) in deep white matter ($x_1 = FA_{deep-WM}$) and in superficial white matter ($x_2 = FA_{super-WM}$) to distinguish the world class gymnasts (WCGs) from the non-athlete normal controls (NCs)

Methods	Variables	Classification			Variables in Eq. 2						Omnibus test			Hosmer–Lemeshow			Model summary		
		Acc	Sens	Spec	β	SE	Wald	*df*	Sig	Exp(β)	χ^2	*df*	Sig	χ^2	*df*	Sig	− 2LL	CS R^2	Na R^2
LR Forward																			
Step 0	β_0	51.9%	0.0%	100.0%	0.07	0.39	0.04	1	0.85	1.08	–	–	–	–	–	–	–	–	–
Step 1	x_1	77.8%	76.9%	78.6%	102.90	42.07	5.99	1	0.01	5.3E + 44	8.64	1	0.003	5.10	7	0.65	28.7	0.27	0.37
	β_0				− 47.74	19.54	5.97	1	0.02	0.00									
Enter																			
Step 0	β_0	51.9%	0.0%	100.0%	0.07	0.39	0.04	1	0.85	1.08	–	–	–	–	–	–	–	–	–
Step 1	x_1	74.1%	69.2%	78.6%	111.51	47.55	5.50	1	0.02	2.6E + 48	8.86	2	0.012	5.45	7	0.61	28.5	0.28	0.37
	x_2				− 21.02	45.45	0.21	1	0.64	0.00									
	β_0				− 43.62	21.18	4.24	1	0.04	0.00									

Two methods were adopted, the Likelihood Ratio (LR) stepwise forward method and the Enter method (see Eq. 2). Step 0 represents no variable but constant term in the regression model. Step 1 included independent variables ($x_1 = FA_{deep-WM}$ or $x_2 = FA_{super-WM}$ or both of them) in the regression model (Eq. 2). β represents regression coefficient and β_0 represents the constant term. Wald is a statistic to depict significance of logistic regression coefficients

SE standard error, *df* degree of freedom, *Sig* significance, − 2*LL* -2loglikelihood, *CS* R^2 Cox & Snell R^2, *Na* R^2 Nagelkerke R^2, *Acc* accuracy, *Sens* sensitivity; *Spec* specificity

SMA and pre-SMA) cortex of the SF with posterior region of IFG (e.g., Tr and Op) and part of frontal longitudinal system (FLS) connecting SF and middle frontal gyrus (MFG). The SFG and MFG partially form a network for gaze control (Anderson et al. 2012) and for initiating and coordinating complex eye, head and arm movements (Catani et al. 2012). The FLS is likely to play a role in coordinating movement planning and execution with an overall goal directed strategy (Catani et al. 2012) and lesions to FLS are likely to manifest with impairment in executive functions, sustained attention and working memory (Stuss et al. 2002). Furthermore, Nazeri et al. showed the FA beneath the IFG (e.g., Tr and Op) and MFG (e.g., RMF) could be used to predict attention and working memory performance and FA extracted from the Op (part of IFG) could be used to predict processing speed performance in healthy people (Nazeri 2013). When it comes to the factors contributing to alteration of FA in super-WM, a previous study (Liu et al. 2016) found diffusion changes in the super-WM did not relate to cortical thinning but relate to large-scale functional network, which suggested a closer relationship between the super-WM and functional changes. Indeed, we explored cortical thickness change in WCGs and did not detect substantial overlap between super-WM and cortical thickness changes, which was consistent with previous studies (Wu et al. 2014, 2016).

Classifications

Both logistic regression (Table 4) and SVM analyses (Table 5) indicated that $FA_{deep-WM}$ could be used to distinguish the two groups at a relative high accuracy independent of $FA_{super-WM}$. Previous studies in gymnasts also implicated training-induced changes in deep-WM tracts (Wang et al. 2013; Huang et al. 2015). Our studies further suggested these plastic changes mainly happened in deep-WM relative to super-WM. Our results from univariate analyses showed effects of both $FA_{super-WM}$ and $FA_{deep-WM}$ on brain plasticity induced by gymnastic training while that of multivariate analyses showed only $FA_{deep-WM}$ played a key role in differentiating the two groups. This discrepancy could be explained by more regionally specific contributions of frontal super-WM to this domain. The super-WM differs from the deep-WM in several ways. For example, super-WM is the last region to myelinate (Bartzokis 2004) and the oligodendrocytes in the super-WM myelinate many axon segments with fewer wraps than in the deep-WM (Butt and Berry 2000), which may lead super-WM more easily to plasticity. Thus, the effects of deep- and super-WM on training-induced brain plasticity may be complex and need to be further investigated.

Table 5 Accuracy, sensitivity, and specificity of the pattern classification analyses derived from the support vector machine (SVM) to distinguish the world class gymnasts (WCGs) from non-athlete normal controls (NCs)

FA map/mask	Accuracy (%)	Sensitivity (%)[a]	Specificity (%)[b]	*p* value
super-WM and deep-WM	74.1	69.2	78.5	0.01
super-WM	51.8	38.5	64.3	–
deep-WM	81.5	84.6	78.6	0.01

super-WM superficial white matter; *deep-WM* deep white matter

[a]Sensitivity was estimated as the percentage of all individuals of the WCGs who were correctly identified as the WCGs

[b]Specificity was estimated as the percentage of all individuals of the NCs who were correctly identified as the NCs

Potential mechanism for reduced FA in gymnasts

Although increase in FA is typically observed in association with learning (Scholz et al. 2009; Keller and Just 2009), we found uniformly decreased FA in deep- and super-WM in the gymnasts due to long-term and intensive gymnastic training. Training time may be an important factor contributing to the direction of FA change. Scholz et al. (2009) found significant training-related increased FA in WM after 6 weeks with five training days per week. They thought the process of electrical activity in an axon regulating its myelination over a time course of days to weeks (Ishibashi et al. 2006; Demerens and Lubetzki 1996) is a potential mechanism for the increased diffusion measures. However, we recruited professional gymnasts who have accepted long-term motor training for more than 10 years. Thus, there is a possibility that the gymnasts in the present study have already went through the initial phase of motor skill learning, which involved neuronal recruitment, and entered a more efficiency phase of motor proficiency. That is, after practicing several hours a day for a number of years, gymnasts seem to be able to coordinate and execute their routines effortlessly (Diedrichsen and Kornysheva 2015). Likewise, several previous studies recruiting professional ballet dancers (Hanggi et al. 2010) and skilled golfers (Jäncke et al. 2009) found decreased FA.

Limitations

The present study provides novel insight regarding subtle white matter plasticity in world class gymnasts, but there are a few issues to note. First, the sample size (total of 13 WCGs) is relatively small, which was necessitated by the small pool of world champion gymnasts available for the study. Small sample size may limit the statistical power for detecting group differences (Button et al. 2013) and relationship between the FA in deep- and super-WM tracts and the training years. Indeed, our correlation analyses did not be carried out through the multiple comparison correction. In addition, we cannot rule out the effects of the possibly lower level of academic training in the gymnasts on brain plasticity, although all the subjects had at least high school level education at the time of this study. Second, our results could not inform about the underlying cellular changes mediating the observed effects. We cannot discern the contributions of myelination, fiber diameter, density, and tissue organization to the FA value. Third, we did not perform a longitudinal study to detect the brain structural changes in these gymnasts. Therefore, we cannot completely rule out the possibility that maturation and/or innate predisposition could have caused or contributed to the differences between the gymnasts and the controls even though we found the brain-behavior correlations. Fourth, we did not include behavioral measures, which may limit the explanatory power of our results. Further studies quantitatively assessing gymnastic skills should be conducted to draw more definitive conclusions about how training and expertise relate to brain white matter plasticity.

In conclusion, long-term intensive gymnastic training could induce regional changes in not only four regional deep white matter tracts but also four U-shaped tracts in the frontal lobe. Our results suggested that the microstructural change appears to have been formed in response to gymnastic training. Furthermore, FA of deep white matter provides higher potential to distinguish the gymnasts from the non-athlete normal controls than that of superficial white matter. A better understanding of the microstructural change of deep and superficial white matter in world class gymnasts will help us to know about the neural basis of motor skill acquisition and development in elite athletes.

Acknowledgements This work was supported by funding from the National Natural Science Foundation of China (Grant Numbers: 81371535, 81271548, 81428013, and 81471654).

Compliance with ethical standards

Conflict of interest We declare that we have no competing financial interests.

Ethical approval All procedures performed in studies involving human participantswere in accordance with the ethical standards of the Institutional Review Board of theState Key Laboratory of Cognitive Neuroscience and Learning at Beijing NormalUniversity (BNU) and with

the 1964 Helsinki declaration and its later amendments orcomparable ethical standards.

Informed consent Informed consent was obtained from all individual participantsincluded in the study.

References

Alexander DC et al (2001) Spatial transformations of diffusion tensor magnetic resonance images. IEEE Trans Med Imaging 20(11):1131–1139

Anderson EJ et al (2012) Cortical network for gaze control in humans revealed using multimodal MRI. Cereb Cortex 22(4):765–775

Barkovich AJ (2000) Concepts of myelin and myelination in neuroradiology. Am J Neuroradiol 21(6):1099

Bartzokis G (2004) Age-related myelin breakdown: a developmental model of cognitive decline and Alzheimer's disease. Neurobiol Aging 25(1):5

Behrens TE et al (2003) Non-invasive mapping of connections between human thalamus and cortex using diffusion imaging. Nat Neurosci 6(7):750–757

Behrens TE et al (2007) Probabilistic diffusion tractography with multiple fibre orientations: what can we gain? Neuroimage 34(1):144–155

Benjamini Y, Hochberg Y (1995) Controlling the false discovery rate—a practical and powerful approach to multiple testing. J Roy Stat Soc 57(1):289–300

Bennett EL et al (1964) Chemical and anatomical plasticity of brain. Science 146(3644):610–619

Bisley JW, Goldberg ME (2003) Neuronal activity in the lateral intraparietal area and spatial attention. Science 299(5603):81–86

Butt A, Berry M (2000) Oligodendrocytes and the control of myelination in vivo: new insights from the rat anterior medullary velum. J Neurosci Res 59(4):477–488

Button KS et al (2013) Power failure: Why small sample size undermines the reliability of neuroscience. Nat Rev Neurosci 14(5):365

Catani M et al (2012) Short frontal lobe connections of the human brain. Cortex 48(2):273–291

Chang CC, Lin CJ (2011) LIBSVM: A library for support vector machines. Acm Trans Intell Syst Technol 2(3):27

IBM Corp (2011) IBM SPSS Statistics for Windows, Version 20.0. IBM Corp, Armonk, NY

Demerens C, Lubetzki C (1996) Induction of myelination in the central nervous system by electrical activity. Proc Natl Acad Sci USA 93(18):9887–9892

Diedrichsen J, Kornysheva K (2015) Motor skill learning between selection and execution. Trends Cogn Sci 19(4):227–233

Draganski B et al (2004) Neuroplasticity: changes in grey matter induced by training. Nature 427(6972):311–312

Fan L et al (2014) Connectivity-based parcellation of the human temporal pole using diffusion tensor imaging. Cereb Cortex 24(12):3365–3378

Filippi M et al (2010) Motor learning in healthy humans is associated to gray matter changes: a tensor-based morphometry study. Plos One 5(4):e10198

Fogassi L, Luppino G (2005) Motor functions of the parietal lobe. Curr Opin Neurobiol 15(6):626–631

Griswold MA et al (2002) Generalized autocalibrating partially parallel acquisitions (GRAPPA). Magn Reson Med 47(6):1202–1210

Grotegerd D et al (2014) MANIA-a pattern classification toolbox for neuroimaging data. Neuroinformatics 12(3):471–486

Halsband U, Lange RK (2006) Motor learning in man: a review of functional and clinical studies. J Physiol Paris 99(4):414–424

Hanggi J et al (2010) Structural neuroplasticity in the sensorimotor network of professional female ballet dancers. Hum Brain Mapp 31(8):(1196–1206)

Hänggi J et al (2015) Structural brain correlates associated with professional handball playing. Plos One 10(4):e0124222

Hartzell JF et al (2016) Brains of verbal memory specialists show anatomical differences in language, memory and visual systems. Neuroimage 131:181–192

Hoeft F et al (2007) More is not always better: increased fractional anisotropy of superior longitudinal fasciculus associated with poor visuospatial abilities in Williams syndrome. J Neurosci 27(44):11960–11965

Hua K et al (2008) Tract probability maps in stereotaxic spaces: analyses of white matter anatomy and tract-specific quantification. Neuroimage 39(1):336–347

Huang R et al (2015) Long-term intensive training induced brain structural changes in world class gymnasts. Brain Struct Funct 220(2):625–644

Ishibashi T et al (2006) Astrocytes Promote Myelination in Response to Electrical Impulses. Neuron 49(6):823–832

Jäncke L et al (2009) The Architecture of the Golfer's Brain. Plos One 4(3):e4785

Jbabdi S, Johansen-Berg H (2011) Tractography: where do we go from here? Brain Connect 1(3):169

Jbabdi S et al (2015) Measuring macroscopic brain connections in vivo. Nat Neurosci 18(11):1546

Jenkinson M, Smith S (2001) A global optimisation method for robust affine registration of brain images. Med Image Anal 5(2):143–156

Jenkinson M et al (2012) Fsl. Neuroimage 62(2):782–790

Johansenberg H, Rushworth MF (2009) Using diffusion imaging to study human connectional anatomy. Annu Rev Neurosci 32(1):75

Johnson RT et al (2014) Diffusion properties of major white matter tracts in young, typically developing children. Neuroimage 88(2):143–154

Jones DK (2010) Diffusion MRI: Theory, Methods, and Applications. Springer, New York, p 371

Karnath HO et al (2004) The anatomy of spatial neglect based on voxelwise statistical analysis: a study of 140 patients. Cereb Cortex 14(10):1164

Keller TA, Just MA (2009) Altering cortical connectivity: Remediation-induced changes in the white matter of poor readers. Neuron 64(5):624–631

Konrad A, Winterer G (2008) Disturbed structural connectivity in schizophrenia—primary factor in pathology or epiphenomenon? Schizophr Bull 34(1):72–92

Landi SM, Baguear F, Della-Maggiore V (2011) One week of motor adaptation induces structural changes in primary motor cortex that predict long-term memory one year later. J Neurosci 31(33):11808–11813

Lebel C et al (2012) Diffusion tensor imaging of white matter tract evolution over the lifespan. Neuroimage 60(1):340

Lerch JP et al (2017) Studying neuroanatomy using MRI. Nat Neurosci 20(3):314

Liu M et al (2016) The superficial white matter in temporal lobe epilepsy: a key link between structural and functional network disruptions. Brain 139(9):2431

Makris N et al (2005) Segmentation of subcomponents within the superior longitudinal fascicle in humans: a quantitative, in vivo, DT-MRI study. Cereb Cortex 15(6):854–869

Maricich S et al (2007) Myelination as assessed by conventional MR imaging is normal in young children with idiopathic developmental delay. AJNR American journal of neuroradiology 28(8):1602–1605

Menon V, Uddin LQ (2010) Saliency, switching, attention and control: a network model of insula function. Brain Struct Funct 214(5):655–667

Nazeri A et al (2013) Alterations of superficial white matter in schizophrenia and relationship to cognitive performance. Neuropsychopharmacology 38(10):1954

Nazeri A et al (2015) Superficial white matter as a novel substrate of age-related cognitive decline. Neurobiol Aging 36(6):2094–2106

Nichols TE, Holmes AP (2002) Nonparametric Permutation Tests For Functional Neuroimaging: A Primer with Examples. Hum Brain Mapp 15(1):1

Oechslin MS et al (2009) The plasticity of the superior longitudinal fasciculus as a function of musical expertise: a diffusion tensor imaging study. Front Human Neurosci 3(1):76

Oishi K et al (2008) Human brain white matter atlas: Identification and assignment of common anatomical structures in superficial white matter. Neuroimage 43(3):447–457

Oishi K et al (2011) Superficially Located White Matter Structures Commonly Seen in the Human and the Macaque Brain with Diffusion Tensor Imaging. Brain Connect 1(1):37–47

Park IS et al (2015) White matter plasticity in the cerebellum of elite basketball athletes. Anatomy Cell Biol 48(4):262–267

Pereira F, Botvinick MM (2009) Machine learning classifiers and fMRI: A tutorial overview. Neuroimage 45(1):S199-S209

Petrides M, Pandya DN (1984) Projections to the frontal cortex from the posterior parietal region in the rhesus monkey. J Comp Neurol 228(1):105–116

Petrides M, Pandya DN (1988) Association fiber pathways to the frontal cortex from the superior temporal region in the rhesus monkey. J Comp Neurol 273(1):52

Phillips OR et al (2013) Superficial white matter: effects of age, sex, and hemisphere. Brain Connect 3(2):146

Pierpaoli C et al (2001) Diffusion tensor MR imaging of the human brain. Radiology 201(3):637

Reveley C et al (2015) Superficial white matter fiber systems impede detection of long-range cortical connections in diffusion MR tractography. Proc Natl Acad Sci USA 112(21):E2820

Schmahmann JD et al (2007) Association fibre pathways of the brain: parallel observations from diffusion spectrum imaging and autoradiography. Brain 130(3):630

Scholz J et al (2009) Training induces changes in white-matter architecture. Nat Neurosci 12(11):1370–1371

Schüz A, Braitenberg V, Miller R (2002) The human cortical white matter: quantitative aspects of cortico-cortical long-range connectivity. In: Schüz A, Miller R (eds) Cortical areas: unity and diversity. Taylor Francis, London, UK, pp 377–385

Sexton CE et al (2016) A systematic review of MRI studies examining the relationship between physical fitness and activity and the white matter of the ageing brain. Neuroimage 131:81–90

Smith SM et al (2006) Tract-based spatial statistics: Voxelwise analysis of multi-subject diffusion data. Neuroimage 31(4):1487–1505

Specht K, Reul J (2003) Functional segregation of the temporal lobes into highly differentiated subsystems for auditory perception: an auditory rapid event-related fMRI-task. Acta Pol Pharm 20(4):1944

Stuss DT, Alexander MP, Floden D, Binns MA, Levine B, Mcintosh AR et al (2002) Fractionation and localization of distinct frontal lobe processes: evidence from focal lesions in humans. In: Stuss DT, Knight RT (eds) Principles of Frontal Lobe Function. pp 392–407

Szeszko PR, Kingsley PB (2010) MRI atlas of human white matter. Concepts Magn Resonan Part A 28A(2):180–181

Taubert M et al (2010) Dynamic properties of human brain structure: learning-related changes in cortical areas and associated fiber connections. J Neurosci 30(35):11670–11677

Umarova RM et al (2010) Structural connectivity for visuospatial attention: significance of ventral pathways. Cereb Cortex 20(1):121–129

Von Der Heide RJ et al (2013) Dissecting the uncinate fasciculus: disorders, controversies and a hypothesis. Brain 136(6):1692

Wakana S et al (2007) Reproducibility of quantitative tractography methods applied to cerebral white matter. Neuroimage 36(3):630–644

Wang B et al (2013) Brain anatomical networks in world class gymnasts: a DTI tractography study. Neuroimage 65(1):476

Wang X et al (2014) White matter microstructure changes induced by motor skill learning utilizing a body machine interface. Neuroimage 88(3):32–40

Wu M et al (2014) Development of superficial white matter and its structural interplay with cortical gray matter in children and adolescents. Hum Brain Mapp 35(6):2806

Wu M, Kumar A, Yang S (2016) Development and aging of superficial white matter myelin from young adulthood to old age: Mapping by vertex-based surface statistics (VBSS). Hum Brain Mapp 37(5):1759

Yeatman JD et al (2012) Tract profiles of white matter properties: automating fiber-tract quantification. PLoS One 7(11):e49790

Yeatman JD, Wandell BA, Mezer AA (2014) Lifespan maturation and degeneration of human brain white matter. Nat Commun 5(5):4932

Zatorre RJ, Fields RD, Johansen-Berg H (2012) Plasticity in gray and white: neuroimaging changes in brain structure during learning. Nat Neurosci 15(4):528–536